Archaeological and Anthropological Sciences (2019) 11:4025–4034
https://doi.org/10.1007/s12520-019-00799-3

ORIGINAL PAPER

First insights into Chinese reverse glass paintings gained by non-invasive spectroscopic analysis—tracing a cultural dialogue

Simon Steger[1] · Diana Oesterle[2,3] · Rupprecht Mayer[4] · Oliver Hahn[1,5] · Simone Bretz[6] · Gisela Geiger[2]

Received: 3 December 2018 / Accepted: 28 January 2019 / Published online: 8 February 2019

Abstract
This work presents a technical investigation of two Chinese reverse glass paintings from the late 19th and early 20th centuries. A multi-analytical, non-invasive approach (X-ray fluorescence (XRF), diffuse reflectance infrared Fourier transform spectroscopy (DRIFTS), Raman spectroscopy) was used to identify the pigments and classify the binding media. The results reveal a combined use of traditional Chinese and imported European materials. Several pigments like cinnabar, lead white, orpiment, carbon black and copper-arsenic green (probably emerald green) were found in both paintings; red lead, artificial ultramarine blue, Prussian blue and ochre appear in at least one of the paintings. The proof of limewash (calcite and small amounts of portlandite) as a backing layer in *Yingying and Hongniang* indicates that clamshell white was also used for reverse glass paintings. Drying oil was classified as a binding media in most areas of both paintings. However, the orange background of *The Archer* yielded prominent bands of both proteinaceous and fatty binder.

Keywords Reverse glass painting · Non-invasive analysis · Pigment identification · XRF · Raman spectroscopy · DRIFTS · Limewash · Emerald green

Introduction

The technique of painting on the reverse side of a glass panel yields characteristic features: (1) the paint layers are applied in reverse order, starting with the front most layer, (2) in contrast to stained glass, it does not involve a firing process and (3) these paintings are viewed in reflected light. Moreover, reverse glass paintings reveal an impressive gloss, luminosity and depth of colour—unattainable with other painting techniques. The history of the Chinese glass painting tradition is directly linked to the availability of high-quality glass sheets. A Dutch East Indian trading company contract, signed in Pattani and dated from 1608, suggests that flat glass and mirrors, probably from Venice, were already exported to southeast China in the early seventeenth century (Mayer 2018 and references therein). In 1699, craftsmen in Canton (Guangzhou) had acquired the technological knowledge to produce high-quality flat glass and were certainly capable of producing their own panels (Curtis 2009). The first European reverse paintings on glass arrived in China in the seventeenth century as gifts and presents from European delegations and salesmen (Mayer 2018). However, no Chinese reverse glass paintings are known from this period. In the mid-eighteenth century, foreigners received restricted permission to conduct trade in Canton where an intensive production of reverse glass paintings had already developed in the preceding years. Due to the lack of historical references, the starting date remains unclear. Oil-based colours were brought to China and were used for decorating glass panels rather than the traditional glue-based water colours (Winter 1984; Curtis 2009). In the eighteenth century,

✉ Simon Steger
simon.steger@bam.de

✉ Rupprecht Mayer
rupprecht_mayer@hotmail.com

1 Federal Institute for Materials Research and Testing (BAM), Division 4.5, Unter den Eichen 44-46, Berlin, Germany

2 Museum Penzberg - Sammlung Campendonk, Am Museum 1, Penzberg, Germany

3 LMU Munich, Institute of Art History, Zentnerstraße 31, Munich, Germany

4 Sinologist, Burghausen, Germany

5 Centre for the Study of Manuscript Cultures, University of Hamburg, Warburgstraße 26, Hamburg, Germany

6 Conservator for Reverse Paintings on Glass, Garmisch-Partenkirchen, Germany

Christian missionaries (Jesuits) came to China and were asked to carry out several reverse glass paintings for the emperor. It was reported that they admired the proficiency and skills of the Chinese artists and learned from them (Van Drongen 2006; Mayer 2018). Reverse glass painters from Canton were sent to Beijing to work in the palace workshops, and at the same time, reverse glass paintings were sent from Canton to the court as gifts from high-ranking officials, which proves the high value of these objects. From ~ 1720 until the mid-nineteenth century, numerous reverse glass paintings carried out in a hybrid Chinese-European style were exported from China to Europe, America and South Asia (Mayer 2018). The paintings became one of the major export articles from China to Europe beginning in the second half of the eighteenth century, a circumstance that fostered a multi-lateral artistic dialogue between China and Europe (Van Drongen 2006; Liu 2016). Several of these paintings exported before 1851 have been preserved in the temples of Bangkok (Patterson 2016). Between 1820 and 1860, the technique spread from Canton throughout all China as the subjects and style were adapted to Chinese taste (Mayer 2018). After the upheavals, wars and destruction of the Cultural Revolution in the twentieth century, reverse glass paintings disappeared from public perception. No public collections and very few private ones have been preserved. The historical reverse glass paintings in the emperor's palace are kept in places inaccessible to visitors (Mayer 2018). In 2015 and 2016, an exhibition of the Central Academy of Fine Arts (CAFA Art Museum, Beijing) introduced the Chinese public to oil paintings—including several reverse paintings on glass from the late Qing dynasty. It seems that the importance of this technique for China's art history is slowly gaining recognition.

Generally, archaeometric research in China has focused mainly on wall paintings (e.g. Zeng et al. 2010; Li et al. 2014; Sultan et al. 2017), cloisonné wares (e.g. Kirmizi et al. 2010; Su et al. 2015), ceramics (e.g. Feng et al. 2008; Tite et al. 2012; Qu et al. 2014; Colomban et al. 2017), dyestuff (De Luca et al. 2016; Tamburini et al. 2018) and archaeological artefacts (e.g. Cheung et al. 2017; Hu 2018). Giaccai and Winter (2005) reported a comprehensive analytical study of seven paintings (a hanging scroll on paper and a hanging scroll on silk), ranging from the fourteenth century to the nineteenth century. Their detailed discussion of the use of different pigments through the ages gives an idea how the painting materials evolved in China. Li et al. (2017) were able to date four paper paintings of Chinese Taoist priests to > 1830 by identifying emerald green and artificial ultramarine blue. Yang et al. (2017) investigated four European reverse glass paintings, which were imported to China in the Qing dynasty. They found pigments like cinnabar, malachite, orpiment, indigo and Prussian blue, as well as oil-based binders. To the best of our knowledge, archaeometric studies of Chinese reverse paintings on glass do not exist in scientific literature. In European art history, scientific research is slowly starting to recognise reverse glass paintings and recently, several archaeometric studies have been published (Hahn et al. 2009; Bretz et al. 2009; Baumer et al. 2009; Baumer and Dietemann 2010; Baumer et al. 2012; Steger et al. 2018).

In this paper, we report the first multi-analytic, non-invasive study of two Chinese reverse glass paintings. The over-arching objectives of this study are (1) to characterise the palette used for this technique in China, (2) to validate the dating by identifying modern pigments and (3) to elaborate a possible influence on reverse glass painters in Europe.

Art historical research on the influence of Chinese reverse paintings on glass on European avant-garde artists lacks systematic studies. However, the strong influence of Southeast Asian and Japanese art (e.g. woodblock print, miniatures, pith paper paintings) on the art and society of the nineteenth and early twentieth century has been highlighted by several exhibitions and publications (Berger 1980; Lambourne 2005; Oh 2006; Salmen 2011). "Japonism"—the study of Japanese artworks was a source of inspiration for European artists. Due to the millennia-long art history of Japan and China, artworks from these countries were not considered "primitivism" (in contrast to artworks from Africa and South America) (Lange 2007). Regarding motifs and forms, a cultural imprint of Asian art on several artworks from the *Blaue Reiter* (blue rider) collective around Gabriele Münter, Wassily Kandinsky, Franz Marc and Heinrich Campendonk can be seen. In the early twentieth century, the revival of the technique of painting on the reverse side of a glass panel can be attributed to these artists (Martin 1996). The high esteem for non-European art is evidenced by several photos of Asian artworks published in their almanac *Der Blaue Reiter* in 1912. Moreover, several *Blauer Reiter* artists bought Asian artworks for their private collections. For example, Franz Marc owned a selection of Chinese pith paper paintings from the nineteenth century (Salmen 2008). Several letters between Marc and Kandinsky also mention Japanese and Chinese artworks (Lankheit et al. 1983). Direct evidence that these artists were also influenced by Chinese reverse paintings on glass still need to be discovered. However, art historical analyses of several *Blaue Reiter* reverse glass paintings indicates a clear Asian influence. Franz Marc's reverse glass painting *Landschaft mit Tieren und Regenbogen* (c. 1911) (Fig. 1) shows stylistic features, attributable to Chinese motifs. Traditional Chinese reverse glass paintings reveal a clear orientation toward the colours of the rainbow (Wappenschmidt 2008). Marc followed this colouristic idea and incorporates the rainbow as a symbol of the connection of nature and cosmos. The vertical format of his painting reminds one of a traditional Asian hanging scroll. Characteristic features of Chinese art are not only the strong symbolism and the mystification of motifs, but also the great variety of painted animals and plants. Marc seems to adopt these iconographical aspects with the visualisation of animals as natural phenomena using the typical rainbow

Fig. 1 Franz Marc, *Landschaft mit Tieren und Regenbogen* (c. 1911), gouache on glass, collage of silver foil and paper, Franz Marc Museum, Kochel am See, Franz Marc Stiftung. Image by Walter Bayer (Munich)

colours. He connects traditional, physical forms with abstracted motifs and strong colours, which are even intensified through the glass (Wappenschmidt 2008).

Materials and Methods

Paintings

The painting *Yingying and Hongniang* (Fig. 2a, b) probably shows a scene from the play "The Story of the Western Wing". A pensive woman (Yingying) is leaning against a table close to an opened book. She is thinking about her love, Zhang Sheng. The second woman (Hongniang, Yingying's maid) seems to gesticulate, while looking at Yingying. The painting (193 × 149 mm) comprises a black frame and a wooden backing board. The sinological interpretation suggests a dating to the second half of the nineteenth century or the beginning of the twentieth century for the painting.

The painting *The Archer* (Fig. 2c, d) shows a woman in red and blue garb who is carrying a bow while looking at a man in a greenish dress. The figures are surrounded by an orange background and a floral border. The painting probably shows a scene from an indeterminable play. The heavily scratched glass surface and the border are hints that this painting (287 × 214 mm) was probably used as a tray. However, the typical deep frame is missing. A wooden back board is used to protect the paint layer. A piece of Chinese newspaper was later added between the wood panel and the painting. Several areas of delaminated paint are visible. The sinological interpretation suggests a dating to the last years of the Qing dynasty (beginning of the twentieth century).

Methods

X-ray fluorescence (XRF)

Elemental analysis was performed using a handheld spectrometer Tracer III-SD (Bruker AXS Microanalysis GmbH), which consists of an electrothermally cooled Xflash SDD detector and an X-ray tube equipped with a rhodium anode. The SDD detector has an energy resolution of about 150 eV, as measured on the manganese Kα peak. The instrument was fixed on a tripod perpendicularly to the paintings, with a working distance of approximately 1 mm, and a spot size of about 10 mm in diameter. The excitation parameters were set to 40 kV and 15 μA, with spectra acquired for 20 s. XRF spectra were collected in open-air conditions, which limits the detection of elements to those with an atomic number of 13 (aluminium) and higher ($Z \geq 13$).

Diffuse reflectance infrared Fourier transform spectroscopy (DRIFTS)

In situ diffuse reflectance spectra were recorded, using a 4100 Exoscan FTIR spectrometer (Agilent) fixed on a tripod perpendicular to the paintings (sample, spectrometer distance ~ 1 mm). In this configuration, the reflected signal is collected within an imaginary cone of 45° around the emission beam, which supports the detection of diffuse reflected light. Specular reflection cannot be fully eliminated, so spectral distortions (e.g. reststrahlen bands) still appear. The instrument is equipped with a ZnSe beam splitter, a Michelson interferometer and a thermoelectrically cooled dTGS detector. The excitation parameters were set to 500 scans with a spectral range of 4000–650 cm^{-1} and a spectral resolution of 4 cm^{-1}. Background calibration was done with a gold reference cap. The Thermo Scientific™ OMNIC™ Specta software

Fig. 2 Photographs of the paintings; *Yingying and Hongniang*, **a** front side, **b** reverse side; *The Archer*, **c** front side, **d** reverse side; The symbol "×" indicates the measured spots. © Simone Bretz

(Version 9.7 Madison, WI, USA) was used for comparison to internal databases.

Raman spectroscopy

Non-invasive Raman measurements were conducted with a Renishaw inVia™ Raman system equipped with two lasers (532 and 785 nm) and a Peltier-cooled CCD detector. The NIR laser (grating 1200 lines/mm; max. power on sample 120 mW) and a 100× long distance lens (Leica) were used for all analyses. The spectral range was set to 100–2300 cm^{-1} with a spectral resolution of ~ 1 cm^{-1}. Various conditions (1–60 s; 2–120 accumulations, 1–20% laser power) were applied for measurements. The Thermo Scientific™ OMNIC™ Specta software (Version 9.7 Madison, WI, USA) was used for spike removal and multi-point baseline subtraction.

Results and Discussion

Yingying and Hongniang

A visual inspection suggests that the preparation of the painting follows the Chinese painting traditions: all human figures were at first outlined with thin black lines and then filled with a combination of different colours applied to different areas of each painting to elaborate the details (Li et al. 2017 and references therein). The reverse side of the painting is covered entirely by a thin, fine-grained, white layer (Fig. 2b). Intense calcium signals in every XRF spectrum indicate the presence of a calcium-bearing pigment (e.g. gypsum, chalk). All measured DRIFT points yielded similar spectra originating from this primer. Intense bands at 878 and 1593 cm^{-1} can be ascribed to out-of-plane bending (ν_2) and antisymmetric stretching (ν_3) vibrations of the carbonate moiety in calcite

($CaCO_3$), respectively. Weaker combination bands are visible at 1792 ($\nu_1+\nu_4$) and 2507 cm^{-1} ($\nu_1+\nu_3$) (Miliani et al. 2012). The intense, sharp band at 3640 cm^{-1} (O–H stretching) originates from portlandite ($Ca(OH)_2$) (Fig. 3a, III), which is a typical residue in limewash (Fernández-Carrasco et al. 2012). High lead content in all XRF spectra (Table 1) suggests the presence of lead white (hydrocerussite, $2PbCO_3 \cdot Pb(OH)_2$). Several Raman spectra showed the typical band at 1051 cm^{-1} (Fig. 3b, I), which originates from symmetric CO_3 stretching of lead white (Bell et al. 1997). Ultramarine blue ($Na_7Al_6Si_6O_{24}S_3$) was identified by means of Raman spectroscopy (Fig. 3b, I) using the intense band at 547 cm^{-1} (stretching of the S_3^- radical ion) (Caggiani et al. 2016). However, it was not possible to clarify if ultramarine blue is synthetic or natural, because sampling was prohibited, and DRIFTS did not yield any signals of ultramarine blue, which can be used for this purpose (Miliani et al. 2008). The red areas yielded intense mercury signals in the XRF spectra, indicating the presence of cinnabar (HgS). Furthermore, typical HgS stretching bands at 245, 284 and 344 cm^{-1} (Fig. 3b, I) are visible in the Raman spectrum (Frost et al. 2002). XRF results of the yellow areas suggest the presence of orpiment (As_2S_3). Raman spectra reveal major bands at 292, 309 and 355 cm^{-1} and several weak bands at 136, 155, 178, 201 and 382 cm^{-1} (Fig. 3b, II), which coincide with orpiment references (Trentelman et al. 1996; Frost et al. 2002). The green area is characterised by intense copper and arsenic peaks in the XRF spectrum, probably originating from emerald green ($Cu(CH_3COO)_2 \cdot 3Cu(AsO_2)_2$). Further verifications by means of Raman spectroscopy failed due to fluorescence problems with both lasers. The presence of carbon black can be assumed, because the black area did not yield any signals (e.g. phosphorous for bone black, $Ca_5(PO_4)_3(OH)$) that can be ascribed to other black pigments. XRF measurements of the glass (i.e. from the front side) show high amounts of calcium and silicon and weak peaks of potassium, iron, strontium, barium and lead. It is worth mentioning that the DRIFT spectra of all measured spots show very similar band patterns. Despite the presence of calcite and portlandite, no signals of any other pigment that yields bands in the mid IR range (e.g. ultramarine, lead white) were detected (Fig. 3a, I). Only the intense bands of drying oil at 1742 (C=O stretching), 2852 and 2926 cm^{-1} (CH_2 stretching) (Steger et al. 2018) are visible, in all spectra. The signals from the oily binder originate from the next layer under the thin limewash primer. We assume that this oily layer, which seems to be free of any pigments, behaves like a varnish and prevents the interaction between the formerly water-rich limewash and the painted layers. The painting itself could even have been made with a water-soluble, proteinaceous binder, which would need this extra oil layer for protection.

The Archer

A synopsis of the results is listed in Table 2. XRF measurements of the glass (i.e. from the front side) show high amounts of calcium and silicon and weak peaks of potassium, manganese, iron, zinc, strontium and barium. Lead white appears as the main white pigment in almost every painted area. The extremely intense lead signals in the XRF spectra of the

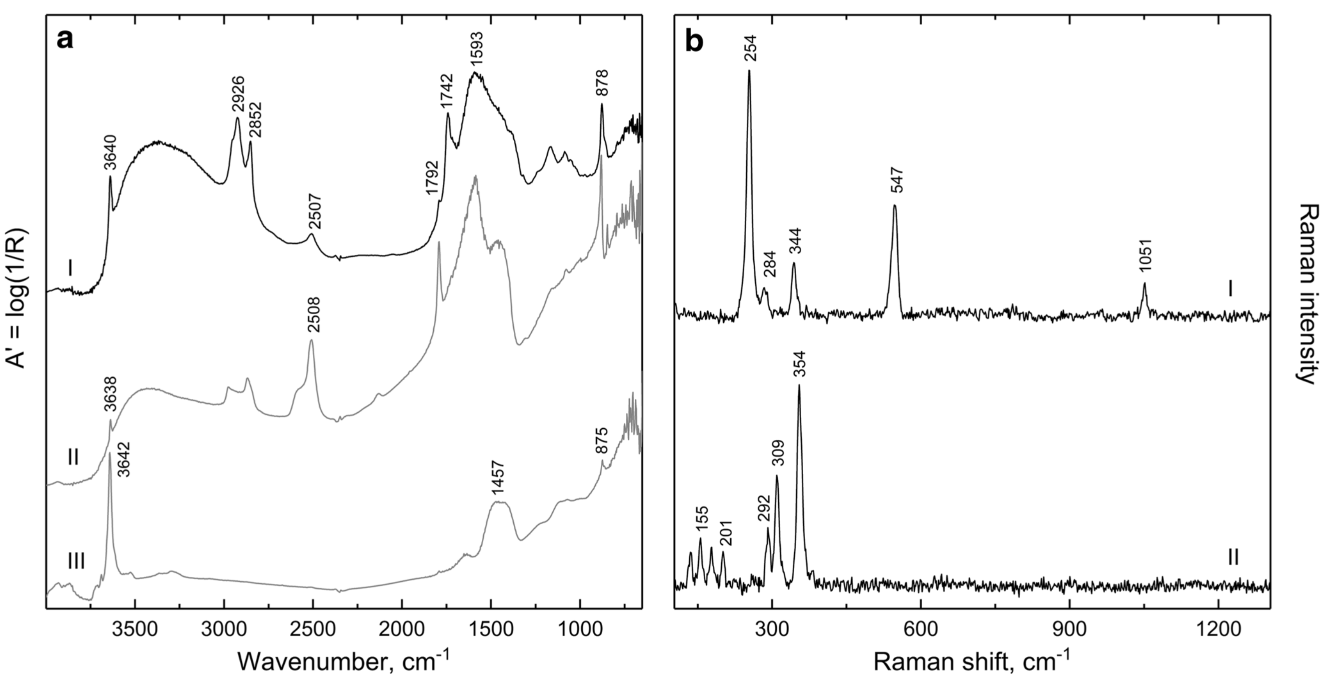

Fig. 3 **a** DRIFT spectrum of spot No. 6 (I); reference spectra of precipitated calcium carbonate with remnants of portlandite (PCC, Fagron; II) and portlandite with remnants of calcite (Fluka; III). **b** Raman spectra of spot No. 12 (I) and No. 9 (II).

Table 1 Summary of results obtained by XRF, Raman spectroscopy and DRIFTS. Analysed areas correspond to the numbered spots in Fig. 2b

No.	Colour	XRF	Raman	DRIFTS
1	White	Pb, Ca	Calcite	Calcite, portlandite, and drying oil
2	Blue	Pb, Ca, (Al, Si, S, Hg)	Ultramarine blue, and lead white	-*
3	Yellow	Pb, Ca, As, (S, Hg)	-	Calcite, portlandite, and drying oil
4	Red	Pb, Ca, Hg	Cinnabar	-
5	Red	Pb, Ca, Hg	-	-
6	Green	Pb, Ca, As, Cu	-	Calcite, portlandite, and drying oil
7	Yellow	Pb, Ca, As, Hg	Orpiment and calcite	-
8	Black	Pb, Ca	-	Calcite, portlandite, and drying oil
9	Yellow	Pb, Ca, As, (S, Hg)	Orpiment	-
10	Blue	Pb, Ca, (Al, Si, S, Hg)	Ultramarine blue and lead white	-
11	Red	Pb, Ca, Hg, (Cu, As)	-	-
12	Blue	Pb, Ca, (Al, Si, S, Hg)	Ultramarine blue, lead white, and cinnabar	Calcite, portlandite, and drying oil

*Not analysed

orange area may also originate from red lead (minium, Pb_3O_4). Raman spectroscopy reveals the presence of red lead by its characteristic bands at 122, 151, 225, 314, 391 and 550 cm^{-1} (Fig. 4b, spectrum III), which are in good agreement with the literature data (Bell et al. 1997; Caggiani et al. 2016). However, the DRIFT spectrum of the same spot shows several lead white bands (Fig. 4a, II), whereas red lead does not absorb in the mid IR range. The sharp band at 1045 cm^{-1} (ν_1; symmetric CO_3 stretching), the inverted band with a minimum at ~ 1392 cm^{-1} (ν_3; antisymmetric stretching), the broad spectral feature at ~ 2435 cm^{-1} (combination band) and the weak O–H stretching band at ~ 3535 cm^{-1} identify lead white properly (Miliani et al. 2012; Steger et al. 2018). The significant darkening of some orange areas (e.g. spot No. 7) can be caused by the degradation of both red lead and lead white (e.g. Goltz et al. 2003; Aze et al. 2008). Multi-spectroscopic measurements of a degraded area yielded no hints of any phase changes (Table 2, No. 7) and further investigations are needed (e.g. XRD). Carbon black was identified in the black areas (Fig. 2d, No. 4, 11) by Raman spectroscopy. The two prominent bands at 1318 and 1599 cm^{-1} (Fig. 4b, II) coincide with the literature data (Coccato et al. 2015). Furthermore, Raman analysis (Fig. 4b, IV) proved the presence of Prussian blue (blue hexacyanoferrate pigment) in the bluish area (Fig. 2d, No. 12) by its characteristic bands at 279, 536 (FeC stretching), 2095 and 2157 cm^{-1} (CN stretching) (Barsan et al. 2011; Samain et al. 2013). The XRF spectrum of the red area (Fig. 2d, No. 8) is dominated by intense mercury signals originating from cinnabar. The brownish areas (Fig. 2d, No. 5, 9, 13) yielded intense arsenic, lead and weaker iron, calcium and silicon peaks in the XRF spectra, suggesting orpiment, lead white and ochre (mainly iron oxides and

Table 2. Summary of results obtained by XRF, Raman spectroscopy and DRIFTS. Analysed areas correspond to the numbered spots in Fig. 2d

No.	Colour	XRF	Raman	DRIFTS
1	Green	Pb, Cu, As, (Si, Ca)	-*	Lead white and emerald green
2	Red	Pb, Hg, (Si, Ca)	Cinnabar	Lead white, chalk, silicates, oxalate and drying oil
3	Orange	Pb	Red lead	Lead white and proteinaceous binder + fatty binder
4	Black	Pb, (Ca, Hg)	Carbon black	-
5	Brown	-	Orpiment	-
6	Red	Pb	Red lead	Lead white and proteinaceous binder + fatty binder
7	White	Pb, (Ca, Hg)	-	-
8	Red	Pb, Hg, (Si, Ca)	Cinnabar	Drying oil
9	Brown	As, (Si, S, K, Ca, Fe, Hg, Pb)	Orpiment	Drying oil and silicates
10	Green	Cu, As, (Si, Ca, Pb)	-	Emerald green, drying oil and oxalate
11	Black	Pb, Ca, (Fe, Hg)	Carbon black	-
12	Blue	Pb, (Si, K, Ca, Fe, Cu)	Prussian blue	Lead white, Prussian blue, chalk, silicates, oxalate and drying oil?
13	Brown	As, Pb, Fe, (Si, K, Ca, Cu)	-	Drying oil, gypsum, silicates and oxalate

*Not analysed

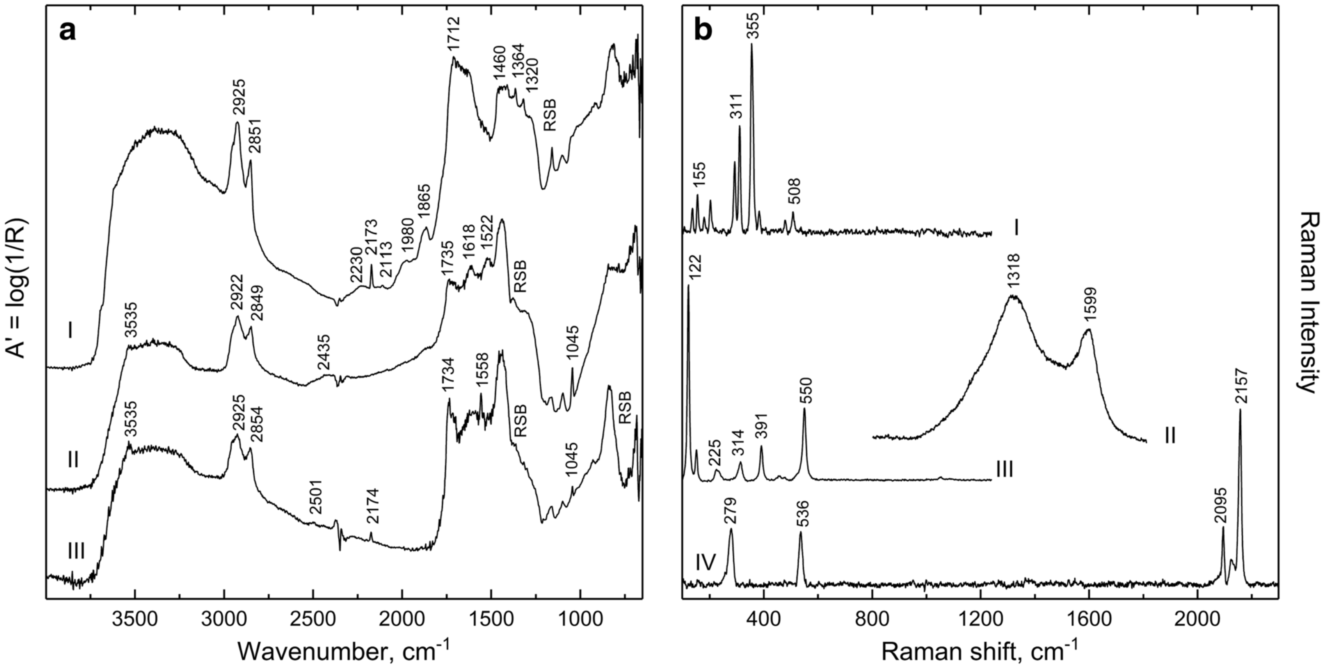

Fig. 4 **a** DRIFT spectra of the brown (spectrum I, spot No. 9), orange (II, No. 3) and green (III, No. 1) areas. **b** Raman spectra of the brown (I, No, 5), black (II, No. 11), orange (III, No. 3) and blue (IV, No. 12) area

hydroxides). Calcium and silicon can also arise from the glass panel. Raman analysis confirmed the presence of orpiment (Fig. 4b, I) by its bands at 137, 155, 180, 203, 292, 354 and 383 cm^{-1} (Trentelman et al. 1996; Frost et al. 2002). The two weak bands at 478 and 508 cm^{-1} probably arise from albite-rich plagioclase, which can naturally appear as relict in clay-rich ochres (Mernagh 1991; Bersani et al. 2018). The DRIFT spectra of the brown areas (Fig. 4a, I) show typical combination bands of silicates in the 1800–2000 cm^{-1} range, but a closer discrimination is not possible. Gypsum ($CaSO_4 \cdot 2H_2O$ was identified by its *reststrahlen* bands with minima at ~1130 and 1205 cm^{-1} (asymmetric SO_4 stretching) and its typical combination bands at 2113 ($\nu_1 + \nu_3$ SO_4) and ~2230 cm^{-1} (bending and libration modes of H_2O) (Miliani et al. 2012; Steger et al. 2018). However, the major signals of the water molecules are absent in the spectrum. The spectra of gypsum and its anhydrous analogue anhydrite ($CaSO_4$) can still be discriminated by the combination band at 2113 cm^{-1}, which is distinctive for gypsum (Miliani et al. 2012). The presence of metal oxalates (1320, 1364 cm^{-1}) can be a hint for the advanced alteration (Monico et al. 2013). The XRF spectra of the green areas (Fig. 2d, No. 1, 10) are dominated by intense copper and arsenic signals. The DRIFT spectra of these areas confirm the presence of emerald green by its bands at 1558 (COO antisymmetric stretching) and 2501 cm^{-1} (Buti et al. 2013). The inverted band with a minimum at ~760 cm^{-1} probably also originates from emerald green, but the assignment of the sharp band at 2173 cm^{-1} (Fig. 4a, III) is not unambiguous. Regarding the binders, drying oil (Fig. 4a, I) could be classified by its characteristic DRIFTS bands at 1460 (CH_2 scissoring), 1712 (C=O stretching), 2851 and 2925 cm^{-1} (CH_2 stretching) (Invernizzi et al. 2017; Steger et al. 2018). A mixture of a proteinaceous (e.g. casein, egg white) and a fatty binder (e.g. drying oil, egg yolk) (Fig. 4a, II) was found in the orange background (Fig. 2d, No. 3, 6). The protein yields characteristic amide II and amide I bands at 1522 and 1618 cm^{-1}, respectively (Steger et al. 2018). The bands at 1735, 2849 and 2922 cm^{-1} indicate the presence of fatty acids.

Discussion

The traditional Chinese palette includes pigments like orpiment, cinnabar, lead white, red lead, iron oxide earths, azurite, malachite, ultramarine blue, clam shell white and several natural dyes (Yu 1988; Wang 2009). Orpiment is spiritually linked to gold and is still used in artworks to this day (Rötter et al. 2007). It was identified in nineteenth century paintings (Wise and Wise 1998) and was exported to England in that time, where it was sold as Chinese yellow (Harley 2001). Large orpiment deposits are located in China (e.g. Hunan) and it is not clear when artificial orpiment was introduced in China (Rötter et al. 2007). In Europe, it was produced at least from the sixteenth century onwards (Rötter et al. 2007; Grundmann et al. 2011). A more precise discrimination between artificial and natural pigment is not possible with the methods used in this study. Cinnabar occurs naturally in large quantities and its synthetic analogue has been produced in China since the sixteenth century by dry process (Fitzhugh et al. 2003). Lead white and red lead have been extensively used in Chinese artwork. The preparation of red lead has been known in China since the fourth century. It was especially used for wall paintings and was less common for paintings on paper and silk (Fitzhugh et al. 2003).

The limewash backing layer of *Yingying and Hongniang* may be a seen as evidence for the use of clam-shell white. Thick, ground seashells (e.g. oysters) are heated over a low fire. The residue (CaO) forms portlandite ($Ca(OH)_2$) when water is continuously added. This water-rich mixture is applied on the painting. Portlandite reacts with atmospheric CO_2 during drying and forms fine-grained calcite ($CaCO_3$) (Yu 1988; Fitzhugh et al. 2003). Clamshell white was important in early Chinese paintings, especially during the Song dynasty where it substituted for chalk (Yu 1988). However, proof of this pigment in artwork is rare. A historical, Chinese recipe from the late seventeenth century reports the preparation procedure (Fitzhugh et al. 2003). Moreover, Yu (1988) states that clamshell white was also used in modern traditional-style paintings. Evidence of other $CaCO_3$ sources (e.g. limestone) for this procedure is non-existent in China but cannot be fully excluded in the late nineteenth century. In Europe, limewash was used only for wall paintings and it has never been identified in reverse paintings on glass.

European salesmen brought new pigments and technologies to China, leading to significant changes in artists' traditional palettes. Examples of this technology transfer are the records of modern, artificial blue and green pigments in the artworks. In Europe, artificial ultramarine blue became commercially available in 1828 and has been exported to China since the late nineteenth century (Plesters 1966; Eremin et al. 2008). Prussian blue reached China already in the second half of the eighteenth century, when it was imported to Canton in large quantities (Eremin et al. 2008). Bailey (2012) suggests, based on historical references, that the Chinese built up their own Prussian blue manufactory in the 1820s. The pigment was found in nineteenth century silk and paper paintings together with azurite and artificial ultramarine (Giaccai and Winter 2005). Emerald green was adopted in China in the late 1840s to early 1850s and was widely used by the third quarter of the nineteenth century, although it was often mixed with malachite rather than used alone (Eremin et al. 2008). Generally, it has been suggested that Foreign Blue and Foreign Green were successful from around 1851 onwards, as they were cheap, convenient to use and gave good results (Yu 1988; Eremin et al. 2008).

It is noteworthy that orpiment was still used in Chinese art production, whereas Western synthetic pigments such as chromates were rarely found in Chinese paintings (Eremin et al. 2008). Lead chromate, for example, was widely used in the nineteenth century in Europe. Due to its toxicity the compound disappeared during the twentieth and was replaced with organic pigments.

Conclusion

The presented results of two reverse glass paintings reveal a combined use of traditional Chinese and imported European materials. Several pigments like cinnabar, lead white, orpiment, carbon black and copper-arsenic green (probably emerald green) were found in both paintings. Drying oil was classified as binder in most areas. However, the DRIFT spectrum of the orange background (*The Archer*) yielded prominent bands from both proteinaceous and fatty binder. The proof of limewash as a backing layer in *Yingying and Hongniang* indicates that clamshell white was also used for reverse glass paintings. The identification of emerald green (*The Archer*) suggests an earliest manufacturing date in the 1830s (Li et al. 2017) and promotes the sinological dating of the painting. Further investigations (e.g. XRD) are needed to identify the copper-arsenic green in *Yingying and Hongniang* and to clarify if the ultramarine blue is either synthetic or natural. Furthermore, systematic scientific and historical research is needed to probe the huge variety of Chinese reverse glass paintings and to elaborate the influence of these paintings on European and Chinese art history.

Acknowledgements We would like to thank Sebastian Simon and Birgit Meng for providing us reference material and background information on limewash and portlandite. We are grateful to Heike Stege for helpful comments on the manuscript.

Funding information The project "Hinterglasmalerei als Technik der Klassischen Moderne 1905–1955" is funded by the Volkswagen-Stiftung, Hannover "Forschung in Museen" reference 89921.

Compliance with ethical standards

Conflict of Interest The authors declare that they have no conflict of interest.

References

Aze S, Vallet JM, Detalle V, Grauby O, Baronnet A (2008) Chromatic alterations of red lead pigments in artwork: a review. Phase Transit 81:145–154

Bailey K (2012) A note on Prussian blue in nineteenth-century Canton. Stud Conserv 57(2):116–121

Barsan MM, Butler IS, Fitzpatrick J, Gilson DFR (2011) High pressure studies of the micro-Raman spectra of iron cyanide complexes: prussian blue ($Fe_4[Fe(CN)_6]_3$), potassium ferricyanide ($K_3[Fe(CN)_6]$), and sodium nitroprusside ($Na_2[Fe(CN)_5(NO)]\cdot 2H_2O$). J Raman Spectrosc 42:1820–1824

Baumer U, Dietemann P (2010) Identification and differentiation of dragon's blood in works of art using gas chromatography/mass spectrometry. Anal Bioanal Chem 397:1363–1376

Baumer U, Dietemann P, Koller J (2009) Identification of resinous materials on 16th and 17th century reverse-glass objects by gas

chromatography/mass spectrometry. Int J Mass Spectrom 284:131–141
Baumer U, Fiedler I, Bretz S, Ranz HJ, Dietemann P (2012) Decorative reverse-painted glass objects from the fourteenth to twentieth centuries: an overview of the binding media. Stud Conserv 57(sup1):9–18. https://doi.org/10.1179/2047058412Y.0000000034
Bell IM, Clark RJH, Gibbs PJ (1997) Raman spectroscopic library of natural and synthetic pigments (Pre- ≈1850 AD). Spectrochim Acta A 53:2159–2179
Berger K (1980) Der Japonismus in der westlichen Malerei 1860–1920 (in German). Prestel, Munich
Bersani D, Aliatis I, Tribaudino M, Mantovani L, Benisek A, Carpenter MA, Gatta GD, Lottici PP (2018) Plagioclase composition by Raman spectroscopy. J Raman Spectros 49:684–698
Bretz S, Baumer U, Stege H, von Miller J, von Kerssenbrock-Krosig D (2009) A German house altar from the sixteenth century: conservation and research of reverse paintings on glass. Stud Conserv 53(4):209–224
Buti D, Rosi F, Brunetti BG, Miliani C (2013) In-situ identification of copper-based green pigments on paintings and manuscripts by reflection FTIR. Anal Bioanal Chem 405:2699–2711
Caggiani MC, Cosentino A, Mangone A (2016) Pigments Checker version 3.0, a handy set for conservation scientists: a free online Raman spectra database. Microchem J 129:123–132
Cheung C, Jing Z, Tang J, Yue Z, Richards M (2017) Examining social and cultural differentiation in early Bronze Age China using stable isotope analysis and mortuary patterning of human remains at Xin'anzhuang, Yinxu. Archaeol Anthropol Sci 9(5):799–816
Coccato A, Jehlicka J, Vandenabeele P (2015) Raman spectroscopy for the investigation of carbon-based black pigments. J Raman Spectrosc 46:1003–1015
Colomban P, Zhang Y, Zhao B (2017) Non-invasive Raman analyses of Chinese huafalang and related porcelain wares. Searching for evidence for innovative pigment technologies. Ceram Int 43:12079–12088
Curtis EB (2009) Glass exchange between Europe and China, 1550-1800: Diplomatic, Mercantile and Technological Interactions. Ashgate, Farnham
De Luca E, Poldi G, Redaelli M, Zaffino C, Bruni S (2016) Multi-technique investigation of historical Chinese dyestuffs used in Ningxia carpets. Archaeol Anthropol Sci 9(8):1789–1798
Eremin K, Stenger J, Huang JF, Aspuru-Guzik A, Betley T, Vogt L, Kassal I, Speakman S, Khandekar N (2008) Examination of pigments on Thai manuscripts: the first identification of copper citrate. J Raman Spectrosc 39:1057–1065
Feng SL, Feng XQ, Zhu JH, Xie GX, Yan LT, Li L, Li G, Shen QH (2008) Nondestructive analysis on ancient porcelain of Longquan Kiln in Zhejiang Province by WDXRF. Chinese. Phys C 32:284–288
Fernández-Carrasco L, Torrens-Martín D, Morales LM, Martínez-Ramírez S (2012) Infrared spectroscopy in the analysis of building and construction materials. In: Theophanides T (ed) Infrared Spectroscopy, Materials Science, Engineering and Technology, Intech, pp 369–382. https://doi.org/10.5772/36186
FitzHugh EW, Winter J, Leona M (2003) Studies using scientific methods: pigments in later Japanese paintings. Freer Gallery of Art Occasional Papers, Washington
Frost RL, Martens WN, Kloprogge T (2002) Raman spectroscopic study of cinnabar (HgS), realgar (As_4S_4), and orpiment (As_2S_3) at 298 and 77K. Neues JB Miner Monat 2002(10):469–480
Giaccai J, Winter J (2005) Chinese painting colors: history and reality. In: Jett P, Winter J, McCarthy B (eds) Scientific Research on the Pictorial Arts of Asia. Archetype Publications, London, pp 99–108
Goltz D, McClelland J, Schellenberg A, Attas M, Cloutis E, Collins C (2003) Spectroscopic studies on the darkening of lead white. Appl Spectrosc 57:1393–1398
Grundmann G, Ivleva N, Richter M, Stege H, Haisch C (2011) The rediscovery of sublimed arsenic sulphide pigments in painting and polychromy: applications of Raman microspectroscopy. In: Spring M (ed) Studying Old Master paintings: technology and practice the National Gallery technical bulletin 30th anniversary conference postprints. Archetype Publications, London, pp 269–276
Hahn O, Bretz S, Hagnau C, Ranz HJ, Wolff T (2009) Pigments, dyes, and black enamel — the colorants of reverse paintings on glass. Archaeol Anthropol Sci 1:263–271
Harley RD (2001) Artists' pigments c.1600-1835, 2nd edn. Archetype Publications, London
Hu Y (2018) Thirty-four years of stable isotopic analyses of ancient skeletons in China: An overview, progress and prospects. Archaeometry 60:144–156
Invernizzi C, Daveri A, Vagnini M, Malagodi M (2017) Non-invasive identification of organic materials in historical stringed musical instruments by reflection infrared spectroscopy: a methodological approach. Anal Bioanal Chem 409:3281–3288
Kirmizi B, Colomban P, Quette B (2010) On-site analysis of Chinese Cloisonné enamels from 15th to 19th century. J Raman Spectrosc 41(7):780–790
Lambourne L (2005) Japonisme. Cultural Crossings between Japan and the West. Phaidon Press, London
Lange B (2007) Konzepte von Bild und Raum: Malerei, Bildhauerkunst, Graphik und Performances (in German). In: Lange B (ed) Vom Expressionismus bis heute. Geschichte der bildenden Kunst in Deutschland (in German), Prestel, Munich, pp 203–250
Lankheit K, Kandinsky W, Marc F (1983) Briefwechsel: mit Briefen von und an Gabriele Münter und Maria Marc (in German). Piper, Munich
Li Z, Wang L, Ma Q, Mei J (2014) A scientific study of the pigments in the wall paintings at Jokhang Monastery in Lhasa, Tibet, China. Herit Sci 2(1):21
Li T, Ji J, Zhou Z, Shi J (2017) A multi-analytical approach to investigate date-unknown paintings of Chinese Taoist priests. Archaeol Anthropol Sci 9:395–404
Liu L (2016) Vitreous Views: Materiality and Mediality of Glass in Qing China through a Transcultural Prism. Getty Res J 8:17–38
Martin P (1996) Hinterglasbilder. Europa - Asien – Afrika (in German). Staatliches Museum für Völkerkunde, Dresden, p 9
Mayer R (2018) Bolihua: Chinese Reverse Glass Painting from the Mei Lin Collection. Hirmer Verlag, Munich
Mernagh TP (1991) Use of the Laser Raman Microprobe for Discrimination Amongst Feldspar Minerals. J Raman Spectros 22:458–457
Miliani C, Daveri A, Brunetti BG, Sgamellotti A (2008) CO_2 entrapment in natural ultramarine blue. Chem Phys Lett 466:148–151
Miliani C, Rosi F, Daveri A, Brunetti BG (2012) Reflection infrared spectroscopy for the non-invasive in-situ study of artists' pigments. Appl Phys A-Mater 106:295–307
Monico L, Rosi F, Miliani C, Daveri A, Brunetti BG (2013) Non-invasive identification of metal-oxalate complexes on polychrome artwork surfaces by reflection mid-infrared spectroscopy. Spectrochim Acta A 116:270–280
Oh MS (2006) Der Blaue Reiter und der Japonismus (in German). PhD thesis, Munich
Patterson JL (2016) Chinese Glass Paintings in Bangkok Monasteries. Arch Asian Art 66(2):153–185
Plesters J (1966) Ultramarine blue, natural and artificial. In: Roy A (ed) Artists' pigments: A handbook of their history and characteristics, vol 2. Oxford University Press, New York, pp 37–65
Qu YA, Xie J, Xi XQ, Huang CJ, Yang JL (2014) Microstructure characteristics of blue-and-white porcelain from the folk kiln of Ming and Qing Dynasties. Ceram Int 40(6):8783–8790
Rötter C, Grundmann G, Richter M, van Loon A, Keune K, Boersma A, Rapp K (2007) Auripigment/orpiment—Studien zu dem Mineral und den künstlichen Produkten. Verlag Anton Siegl, Munich
Salmen B (2008) Chinesische Bilder. Volkskunst für den "Blauen Reiter" (in German). Schloßmuseum Murnau, Murnau

Salmen B (2011) "... diese zärtlichen, geistvollen Phantasien..." Die Maler des "Blauen Reiter" und Japan (in German). Schloßmuseum Murnau, Murnau

Samain L, Grandjean F, Long GJ, Martinetto P, Bordet P, Strivay D (2013) Relationship between the Synthesis of Prussian Blue Pigments, Their Color, Physical Properties, and Their Behavior in Paint Layers. J Phys Chem C 117:9693–9712

Steger S, Stege H, Bretz S, Hahn O (2018) Capabilities and limitations of handheld diffuse reflectance infrared Fourier transform spectroscopy (DRIFTS) for the analysis of colourants and binders in 20th-century reverse paintings on glass. Spectrochim Acta A 195:103–112

Su Y, Qu L, Duan H, Tarcea N, Shen A, Popp J, Hu J (2015) Elemental analysis-aided Raman spectroscopic studies on Chinese cloisonné wares and Painted enamels from the Imperial Palace. Spectrochim Acta A 153:165–170

Sultan S, Kareem K, He L, Simon S (2017) Identification of the authenticity of pigments in ancient polychromed artworks of China. Anal Methods 9:814–825

Tamburini D, Cartwright CR, Pullan M, Vickers H (2018) An investigation of the dye palette in Chinese silk embroidery from Dunhuang (Tang dynasty). Archaeol Anthropol Sci. https://doi.org/10.1007/s12520-017-0592-4

Tite MS, Freestone IC, Wood N (2012) An investigation into the relationship between the raw materials used in the production of Chinese porcelain and stoneware bodies and the resulting microstructures. Archaeometry 54:37–55

Trentelman K, Stodulski L, Pavlovski M (1996) Characterization of Pararealgar and Other Light-Induced Transformation Products from Realgar by Raman Microspectroscopy. Anal Chem 68:1755–1761

Van Drongen PLF (2006) Sensitive plates: nineteen Chinese Paintings on Glass from the End of the Eighteenth Century. Museum Volkenkunde, Leiden, pp 1–61

Wang J (2009) A search for the provenance of natural ultramarine blue as a blue pigment in ancient Chinese art. Wenbo 2009(6):396–402 (in Chinese)

Wappenschmidt F (2008) Bunt leuchtende Bilder der chinesischen Volkskunst – Malereien auf Seide, Papier, Markpapier und hinter Glas (in German). In: Salmen B (ed) Chinesische Bilder. Volkskunst für den "Blauen Reiter" (in German). Schloßmuseum Murnau, Murnau

Winter J (1984) Natural adhesives in East Asian paintings. Stud Conserv 29(sup1):117–120. https://doi.org/10.1179/sic.1984.29.Supplement-1.117

Wise D, Wise A (1998) Observations on nineteenth-century Chinese pigments with special reference to copper greens. In: Eagan J (ed) IPC Conference Papers, 6–9 April 1997. Institute of Paper Conservation, London, pp 125–136

Yang B, Li G, Qu L, Zhao C, Ma H, Ma Q, Chen K (2017) Qinggong Caihui Bolihua Chubu Kexue Fenxi Yanjiu (清宫彩绘玻璃画初步科学分析研究). Zhongguo Wenwu Kexue Yanjiu (中国文物科学研究) 2017(3):72–79 (in Chinese)

Yu F (1988) Chinese painting colours: studies of their preparation and application in traditional and modern times (trans., J. Silbergeld and A. McNair). University of Washington Press, Washington

Zeng QG, Zhang GX, Leung CW, Zuo J (2010) Studies of wall painting fragments from Kaiping Diaolou by SEM/EDX, micro Raman and FT-IR spectroscopy. Microchem J 96:330–336